Published in final edited form as:
Mol Biosyst. 2009 May ; 5(5): 529–541. doi:10.1039/b819502a.

Targeted Lipidomic Analysis of Oxysterols in the Embryonic Central Nervous System

Yuqin Wang[1,*], **Kyle M. Sousa**[2,*], **Karl Bodin**[2,*], **Spyridon Theofilopoulos**[2], **Paola Sacchetti**[2], **Martin Hornshaw**[3], **Gary Woffendin**[3], **Kersti Karu**[4], **Jan Sjövall**[2], **Ernest Arenas**[2], and **William J. Griffiths**[1,‡]

[1]Institute of Mass Spectrometry, School of Medicine, Grove Building, Swansea University, Singleton Park, Swansea SA2 8PP, UK.

[2]Laboratory of Molecular Neurobiology and Department of Medical Biochemistry and Biophysics, Karolinska Institutet, Stockholm SE-17177, Sweden.

[3]Thermo Fisher, Stafford House, Boundary Way, Hemel Hempstead, HP2 7GE, UK.

[4]The School of Pharmacy, University of London, 29-39 Brunswick Square, London WC1N 1AX, UK.

Summary

In this study two regions of embryonic (E11) mouse central nervous system (CNS) have been profiled for their unesterified sterol content. Using high-performance liquid chromatography (HPLC) – mass spectrometry (MS) and tandem mass spectrometry (MS^n) low levels of oxysterols (estimated 2 – 165 ng/g wet weight) were identified in cortex (Ctx) and spinal cord (Sc). The identified oxysterols include 7α-, 7β-, 22R-, 24S-, 25- and 27-hydroxycholesterol; 24,25- and 24,27-dihydroxycholesterol; and 24S,25-epoxycholesterol. Of these, 24S-hydroxycholesterol is biosynthesised exclusively in brain. In comparison to adult mouse where the 24S-hydroxycholesterol level is about 40 μg/g in brain the level of 24S-hydroxycholesterol reported here (estimated 26 ng/g in Ctx and 13 ng/g in Sc) is extremely low. Interestingly, the level of 24S, 25-epoxycholesterol in both CNS regions (estimated 165 ng/g in Ctx and 91 ng/g in Sc) is somewhat higher than the levels of the hydroxycholesterols. This oxysterol is formed in parallel to cholesterol via a shunt of the mevalonate pathway and its comparatively high abundance may be a reflection of a high rate of cholesterol synthesis at this stage of development. Levels of cholesterol (estimated 1.25 mg/g in Ctx and 1.15 mg/g in Sc) and its precursors were determined by gas chromatography – mass spectrometry (GC-MS). In both CNS regions cholesterol levels were found to be lower than those reported in the adult, but in relation to cholesterol the levels of cholesterol precursors were higher than found in adult indicating a high rate of cholesterol synthesis. In summary, our data provide evidence for the presence of endogenous oxysterols in two brain regions of the developing CNS. Moreover, while most of the enzymes involved in hydroxysterol synthesis are minimally active at E11, our results suggest that the mevalonate pathway is significantly active, opening up the possibility for a function of 24S,25-epoxycholesterol during brain development.

Introduction

In recent years there has been increasing interest in the sterol profiles of mammalian brain1. This interest has been driven by two key factors; (i) the in *vitro* activity of many cholesterol

‡Corresponding author..
*Authors contributed equally.

Europe PMC Funders Author Manuscripts

(C^5-3β-ol) metabolites and precursors as ligands to the liver X receptors (LXRs)2-5; and (ii) the activity of many of these molecules as inhibitors of cholesterol synthesis via interaction through INSIGs (insulin-induced genes) or SCAP (SREBP cleavage-activating protein) with SREBP-2 (sterol regulatory element-binding protein-2) processing, or through interaction involving INSIG leading to HMG-CoA (hydroxymethylglutaryl-CoA) reductase degradation (see Figures 2 and 5 in reference 6)6,7.

The LXRs are members of the nuclear receptor superfamily involved in the transcriptional regulation of many of the genes involved in lipid homeostasis8. The most potent endogenous ligands to LXRs are oxysterols e.g. 24S-hydroxycholesterol (C^5-3β,24S-diol), 24S,25-epoxycholesterol (C^5-3β-ol-24S,25-epoxide), 24-oxocholesterol (C^5-3β-ol-24-one) and 27-hydroxycholesterol (C^5-3β,27-diol)3,4, and cholesterol precursors e.g. desmosterol ($C^{5,24}$-3β-ol), are also active (see Figure 1 and supplementary Figure S1 for sterol structures). LXRβ is broadly expressed in the developing and adult rodent brain9,10. In the adult LXRα,β double-knockout mouse Wang et al have observed that the lateral ventricles are closed, the ependymal cells lining the ventricles accumulate lipid droplets, and there is neuronal loss and astrocyte proliferation11. Further, male LXRβ−/− mice suffer from adult-onset motor neuron degeneration12,13.

The expression of enzymes of the cholesterol biosynthetic pathway are regulated by SREBP-26,14. SREBP-2 is synthesised in the endoplasmic reticulum (ER), and is escorted to the Golgi complex by SCAP. In the Golgi complex SREBP-2 is proteolytically cleaved to release the transcriptionally active form of the protein nSREBP-2 (see Figure 3 in reference 6). In cells affluent in cholesterol the SCAP-SREBP-2 complex associates with an ER resident protein INSIG, and the SCAP-SREBP-2 complex is retained in the ER. Reduction of cellular cholesterol leads to dissociation of the SCAP-SREBP-2 complex from INSIG and transport to the Golgi for processing of SREBP-2 to its active form (nSREBP-2). While cholesterol interacts with SCAP to cause a conformational change which results in SCAP binding to INSIG and maintenance of SREBP-2 in the ER15,16, oxysterols interact with INSIG to provide the same effect7,17. HMG-CoA reductase is the first committed enzyme in the mevalonate pathway and its expression is regulated at the transcriptional level by SREBP-2 (Figure 1). Remarkably, its degradation is also regulated by a sterol-accelerated mechanism6,18. Lanosterol (4,4,14-Me_3-5α-$C^{8(9),24}$-3β-ol), a precursor of cholesterol, triggers binding of HMG-CoA reductase to INSIG, leading to ubiquitination of the reductase and subsequent degradation. Cholesterol is a much weaker inducer of reductase degradation than lanosterol but the oxysterol 27-hydroxylanosterol (4,4,14-Me_3-5α-$C^{8(9),24}$-3β,27-diol) is the most potent sterol inducer found to date19.

In human about one quarter of the body's free cholesterol is found in brain, and almost all is synthesised *de novo* and in *situ* from acetyl CoA20. Much of the cholesterol in brain goes to make up the myelin sheaths coating axons and as such is turned over at a very slow rate (half life of brain cholesterol in adult rats 2 – 4 months)21. In the developing brain, before the blood brain barrier (BBB) is fully developed cholesterol and its metabolites derived from the mother or foetus can freely enter the brain via the circulation. However, after the barrier is sealed cholesterol must be synthesised in *situ*. Recent data from a study on the 3β-hydroxysterol Δ^7 reductase (Dhcr7) knockout mouse indicates that the BBB is formed at day 10 – 11 (E10-11) after which the brain rapidly becomes the source of its own sterols22. Tint and colleagues also found that the activity of sterol 24,25-reductase (Dhcr24) in brain was low in young foetuses but increased rapidly after E11-12, while in early foetal brain the expression of cholesterol 24-hydroxylase (CYP46A1) was low until E18. Thus, current evidence indicate that most of the cholesterol required for growth and differentiation of the central nervous system (CNS) after E10 - E11 comes from *de novo* synthesis in the brain, and suggest the possibility that some of that cholesterol could be the source of oxysterols.

Unlike cholesterol, oxysterols can cross the BBB and are both exported from and imported to the brain21,23. In the adult continued cholesterol synthesis throughout life requires the existence of an export mechanism, this is provided by oxidation of cholesterol by CYP46A1 to 24S-hydroxycholesterol, which by virtue of the extra hydroxyl group can transverse the BBB21. CYP46A1 is expressed exclusively in brain, normally in neurons24, and in neonates appears to have low activity, which is greatly increase after birth, probably in response to increased cholesterol availability25,26. Interestingly, although in adult mouse the spinal cord synthesises cholesterol at a rate 5-fold higher than other areas of brain, cholesterol is only 2-fold more abundant in this region27. However, the expression of CYP46A1 is less in spinal cord than brain24. A second mechanism for cholesterol export from the CNS thus appears to be operable in spinal cord.

In contrast to CYP46A1, the enzyme responsible for 27-hydroxyation of cholesterol, CYP27A1, is expressed ubiquitously, and in adults 27-hydroxycholesterol appears to be a net import product into brain23. Other oxysterols identified in adult brain include 4β-hydroxycholesterol (C^5-3β,4β-diol) in mouse1, 20S-hydroxycholesterol (C^5-3β,20S-diol) in rat28, 22R-hydroxycholesterol (C^5-3β,22R-diol) in human29, 24-oxocholesterol (C^5-3β-ol-24-one) and 7α,25-, 7α,27-, 24,25-, 24,27- and 25,27-dihydroxycholesterols (C^5-3β,7α,25-triol, C^5-3β,7α,27-triol, C^5-3β,24,25-triol, C^5-3β,24,27-triol, C^5-3β,25,27-triol) in rat30, and 24,25- and 5,6-epoxycholesterols (C^5-3β-ol-24,25-epoxide, C-3β-ol-5,6-epoxide) in mouse1. CYP46A1 has 25- and 27-hydroxylase activity as well as its major 24-hydroxylase activity31, while CYP7B1 which is also expressed in brain has 7α-hydroxylase activity towards 25-hydroxycholesterol (C^5-3β,25-diol) and 27-hydroxycholesterol32,33. Zhang and colleagues demonstrated this in cultures of foetal rat astrocytes and were able to identify 7α,25- and 7α,27-dihydroxycholesterols; 7α,25- and 7α,27-dihydroxycholest-4-en-3-ones (C^4-7α,25-diol-3-one, C^4-7α,27-diol-3-one); 3β,7α-dihydroxycholest-5-en-27-oic acid (CA^5-3β,7α-diol) along with 7α-hydroxy-3-oxocholest-4-en-27-oic acid (CA^4-7α-ol-3-one) from incubations of 25-, and 27-hydroxycholesterols32. In contrast to CYP7B1, CYP7A1 the enzyme responsible for hydroxylation of cholesterol itself is expressed exclusively in liver34.

20S- and 22R-hydroxycholesterols, also identified in brain28,29, are potential intermediates or side-products in the formation of pregnenolone from cholesterol in a reaction catalysed by CYP11A1 ($P450_{scc}$) part of the neurosteroid biosynthetic pathway operating in brain35. Interestingly, 20S-hydroxycholesterol is also found in human placenta28, and 20,22-dihydroxycholesterol (C^5-3β,20,22-triol) sulphate in meconium36. Like 24S- and 27-hydroxycholesterols, 22R-hydroxycholesterol is a potent LXR ligand3, and also inhibits SREBP-2 cleavage by binding to INSIG7. 24S,25-Epoxycholesterol, unlike hydroxycholesterols, is not a cholesterol metabolite but is produced in a shunt of the mevalonate pathway that also produces cholesterol (Figure 1)37-39. 24S,25-Epoxycholesterol is formed by the action of squalene epoxidase on 2,3-monoepoxysqualene (2,3-oxidosqualene) prior to cyclisation by oxidosqualene:lanosterol cyclase (lanosterol synthase, 2,3-oxidosqualene cyclase, OSC), resulting in a final 24S,25-epoxide of cholesterol rather than cholesterol itself (Figure 1). 24,25-Epoxycholesterol is both a ligand to the LXRs and an inhibitor of SREBP-2 processing3,7. It is suggested that its role is to provide an early warning system for newly synthesised cholesterol, to protect the cell against accumulated cholesterol, and to fine tune acute control of cellular cholesterol homeostasis39. As 24S,25-epoxycholesterol is synthesised in the ER it will enable the retention of the INSIG-SCAP-SREBP-2 complex in the ER before newly synthesised cholesterol accumulates to sufficient levels to be “sensed” by SCAP and take over this function. 24S,25-Epoxycholesterol has also been shown to accelerate HMG-CoA reductase degradation in a manner similar to that of other side-chain oxidised cholesterol derivatives. Wong et al have shown that both astrocytes and neurons can synthesise 24S,25-

epoxycholesterol, and by performing experiments on primary human brain cells they were able to show that 24S,25-epoxycholesterol can modulate LXR and SREBP-2 target gene expression38. Data from incubations with [1-^{14}C]-acetate indicate that the rate of synthesis of 24S,25-epoxycholesterol in astrocytes is about 0.3% that of cholesterol, while in neurons the rate of synthesis of 24S,25-epoxycholesterol is an order of magnitude lower38.

Of the above oxysterols many have been found in the circulation at measurable levels, e.g. in human 7α- (C^5-3β,7α-diol, ~40 ng/mL) and 25-hydroxycholesterol (~3 ng/mL), both of which can be formed enzymatically or by autoxidation; 7β-hydroxycholesterol (C^5-3β,7β-diol, ~5 ng/mL), cholestane-3β,5α,6β-triol (C-3β,5α,6β-triol, ~10 ng/mL), and 5,6-epoxycholesterols (~10 ng/mL) which are autoxidation products of cholesterol; and the enzymatically formed oxysterols 24S- (~60 ng/mL) and 27-hydroxycholesterols (~150 ng/mL), 7α,27-dihydroxycholesterol (~10 ng/mL), 7α-hydroxycholest-4-en-3-one (C^4-7α-ol-3-one, ~ 12 ng/mL), and 3β-hydroxycholest-5-en-27-oic (CA^5-3β-ol, ~100 ng/mL), 3β,7α-dihydroxycholest-5-en-27-oic (30 ng/mL) and 7α-hydroxy-3-oxocholest-4-en-27-oic (85 ng/mL) acids40-43. Additionally, 3β,5β-dihydroxy-B-norcholestane-6β-carboxyaldehyde (4 ng/mL), the aldol of 3β-hydroxy-5-oxo-5,6-*seco*cholestan-6-al (5,6-*seco*-sterol) has also been identified in human blood41,44. The levels of oxysterols in the rodent circulation are less well studied although where identified the concentrations are mostly of the same order of magnitude as in man45,46. There is, however, no data available on the levels of oxysterols at early stages of embryonic development. We therefore set to examine the levels and profile of oxysterols in the cortex (Ctx) and spinal cord (Sc) at E11, using a very sensitive combination of high-performance liquid chromatography (HPLC) and tandem mass spectrometry (MS/MS or MS^n).

Sterols are traditionally analysed by gas chromatography – mass spectrometry (GC-MS) as trimethylsilyl (TMS) ethers47. GC-MS offers the advantages of a reproducible retention index (RI), structurally informative fragmentation when using electron ionisation (EI) and the existence of extensive spectral libraries47. Oxysterols are also analysed by GC-MS48,49, but here the absence of a molecular ion can lead to confusion in compound identification, particularly in respect to unknowns31,47. As an alternative to GC-MS, LC-MS/MS is gaining prominence1,50-53. Although LC retention times are now highly reproducible, the lack of an accepted retention time index makes the translation of data between laboratories difficult. Further, oxysterols tend to dehydrate upon atmospheric pressure ionisation (API)1, leading to a similar problem to that encountered in GC-MS with respect to molecular weight determination. Additionally, the lack of a basic or acidic group in most oxysterols leads to a low cross-section for ionisation by both electrospray (ES) and atmospheric pressure chemical ionisation (APCI). To circumvent this problem oxysterols in particular, and sterols in general, can be derivatised with charge-carrying groups so as to enhance ion yields upon API i.e. charge-tagging30,54, this also increases their solubility in the mobile phase for reversed-phase chromatography and hence facilitates their analysis by LC-MS/MS.

Here we report the use of both GC-MS and LC-MS^n for the analysis of sterols and oxysterols in different regions of developing mouse CNS.

Results

GC-MS Analysis of Unesterified Sterols and Oxysterols

Full scan EI mass spectra were recorded, and spectra of all peaks in the total ion chromatograms (TIC) evaluated. Reconstructed ion chromatograms (RIC) were generated for all relevant sterol/oxysterol related *m/z* values. The spectra derived from the resultant peaks were assessed. The combined information allowed complete or partial identification

of the compounds present (see Table 1). Quantitative estimates were made by analysing a known amount of lathosterol (5α-C^{7}-3β-ol) TMS ether and comparing peak heights in the TIC.

Sterols—GC-MS analysis was performed on both sterol and oxysterol fractions isolated by chromatography on a Unisil column (fractions U1 and U2 respectively, see supplementary Figure S2). Due to the high level of sterols in the samples there was some tailing of the sterols from fraction U1 into the oxysterol fraction U2. However, oxysterols were found exclusively in fraction U2. Of the sterols identified the amount of cholesterol (estimated 1.25 mg/g Ctx and 1.15 mg/g Sc wet weight) was considerably lower than that reported in adult mouse brain (20 mg/g)20,55, but in good agreement with other data on E11-12 mouse brain (total sterols <1 mg/g)22. In the adult mouse brain the ratios of desmosterol to cholesterol, and lathosterol to cholesterol are usually of the order of 0.00155, although at birth the lathosterol to cholesterol ratio is much higher (0.035)26. Our data on E11 embryonic mouse brain give ratios of 0.03 – 0.01 and 0.01 respectively (Table 1). Both desmosterol and lathosterol are precursors of cholesterol (Figure 1) and their elevated levels relative to cholesterol indicate a high rate of cholesterol synthesis56. This would be in agreement with the data of Tint et al that indicates that after E10-11 the foetal brain is the major source of its own cholesterol22. An additional sterol-like peak was identified in the TIC of both embryonic CNS regions and based on the EI fragment pattern it was assigned to lathosterol with an additional double bond in the side-chain, probably Δ^{24} (5α-$C^{7,24}$-3β-ol) or zymosterol (5α-$C^{8(9),24}$-3β-ol). However, in the absence of an authentic standard we were unable to confirm this identification (see Figure 1). Campesterol (24-Me-C^{5}-3β-ol) and sitosterol (24-Et-C^{5}-3β-ol) are plant sterols and may be present in brain with a dietary origin55; alternatively, their detection may be a result of laboratory contamination of the samples with rubber derived materials57, although we have avoided this as far as possible by performing sample preparation in glass plates, using metal tools, and storage of samples in glass vials. In our study the ratios of campesterol, sitosterol and lanosterol (a normal endogenous precursor of cholesterol, but also a plant sterol) to cholesterol were about 0.005, 0.002, and 0.002 respectively. For comparison, the ratios of campesterol and sitosterol to cholesterol in adult mouse determined in an earlier study were 0.001 and 0.0003 respectively55.

Oxysterols—GC-MS analysis of the sterol and oxysterol fractions (Unisil fractions U1 and U2 respectively, see supplementary Figure S2) allowed the identification of the most abundant oxysterols (Table 1). The limit of detection of the instrument used was approximately 0.2 μg/g wet weight of tissue which precluded the identification of low abundance oxysterols. However, the pattern of oxysterols identified was essentially similar in both CNS regions. The 5,6-epoxycholesterol isomers (5α,6α- and 5β,6β-) were present at a low level (0.8 – 3 μg/g) indicating a minimum of autoxidation during sample preparation. The RICs characteristic of TMS ethers of oxysterols showed several peaks but the spectra were too weak to permit identification of the sterols. Two oxysterols were partially characterised based on their EI fragmentation pattern (Table 1). One was a cholestanediol (C-3,x-diol) and the other a cholestenediol which was found exclusively in the spinal cord fraction and at a higher level than other oxysterols. The EI spectrum of its TMS ether was compatible with a hydroxycholesterol (C^{5}-3,x-diol) with a saturated side-chain and the second hydroxyl group in the A or B ring, but not at C-1, or C-7. As discussed above, it is tempting to speculate that this hydroxycholesterol represents a metabolite (and perhaps export form) of cholesterol from the spinal cord.

LC-MS^n Analysis of Unesterified Sterols and Oxysterols

Preliminary Studies—An initial investigation was performed by capillary-LC-ES-MS^n using the LCQ ion-trap mass spectrometer to evaluate the oxysterol content of Unisil fraction U2 prior to more detail studies on the Orbitrap instrument (see below). Miniaturisation of chromatography from a conventional (2.1 mm i.d.) to capillary (180 μm i.d.) column format with the commensurate reduction in flow-rate (200 → <1 μL/min) provides an increase in concentration of analyte in an eluting peak. As ES is a concentration dependent process this leads to an increase in mass spectrometric sensitivity. Further enhancement in sensitivity was achieved by incorporating a charge-tag on the oxysterol analytes by oxidisation/derivatisation (See supplementary Figure S3). The Girard P (GP) charge-tag offers additional advantages in that: (i) it is specific to compounds possessing a carbonyl group, or in the case of most sterols and oxysterols those oxidised to posses one, (ii) it directs the fragmentation of the resulting $[M]^+$ ion in the MS^2 event, predominantly giving $[M-79]^+$ and $[M-107]^+$ ions (loss of pyridine and pyridine plus CO, respectively, see supplementary Figure S3), so that (iii) MS^3 can be performed on ions specifically formed from the GP-containing $[M]^+$ ion, giving an extra dimension of separation, and that (iv) MS^3 spectra contain a wealth of structure specific information (see supplementary Figure S3 for fragmentation patterns).

By comparing analyte retention time, MS^2 ($[M]^+\rightarrow$), and MS^3 ($[M]^+\rightarrow[M-79]^+\rightarrow$) spectra of components eluting from the reversed-phase column with authentic standard it was possible to identify the presence, and estimate the quantity, of desmosterol, cholesterol, campesterol, 7α-, 7β-, and 24S-hydroxycholesterol; 6β-hydroxycholest-4-en-3-one (C^4-6β-ol-3-one), 24-oxocholesterol; 24,25-dihydroxycholesterol; and 24S,25-epoxycholesterol in the CNS samples (see supplementary Table S1). The close elution of 24S-, 25- and 27-hydroxycholesterol standards from the capillary column made unequivocal confirmation of their presence in CNS difficult, although MS^3 spectra suggested the presence of 25-hydroxycholesterol in addition to 24S-hydroxycholesterol. Similarly, it was not clear if 24,27-dihydroxycholesterol accompanied the 24,25-dihydroxy isomer. To clarify these uncertainties and to obtain a better estimate of quantities, samples were subsequently analysed on the LTQ-Orbitrap.

The sensitivity of the current method is such that the equivalent of <0.2 mg of CNS was injected on column corresponding to low pg amounts of oxysterol analysed. However, the method relies on the analysis of sterols and oxysterols that are first oxidised with cholesterol oxidase to generate 3-oxo groups which are subsequently derivatised with the GP reagent (see supplementary Figure S3). LC-MS^n is then performed on the GP derivatives. The structures of the sterols and oxysterols in CNS are then inferred from the retention times and MS^n spectra of the derivatives with reference to authentic standards. As used in the present study, the method is unable to differentiate between a sterol containing a 3-oxo group before treatment with cholesterol oxidase and one oxidised by cholesterol oxidase to contain one (differentiation could, however, be achieved by repeating the procedure in the absence of cholesterol oxidase). As most known oxysterol have a 3β-hydroxyl group rather than a 3-oxo group we infer that the sterols detected have this function prior to oxidation/derivatisation. This may not be true in the case of e.g. 7α-hydroxycholesterol and 7α-hydroxycholest-4-en-3-one as both oxysterols are known to be present in mammals42. In this case our identification is of the oxysterol and/or its 3-oxo-4-ene metabolite.

In this LC-MS^n study we have paid maximum attention to the identification of oxysterols in cortex and spinal cord, as such the oxidation/derivatisation and sample preparation methods have been optimised for these compounds. The oxidation reaction is only applicable to substrates with a 3β-hydroxy-5-ene or 3β-hydroxy-5α-hydrogen function58, and reaction conditions have been tested so as to give quantitative conversion of 3β-hydroxy-5-ene

oxysterols to their 3-oxo-4-ene analogues (see supplementary Figure S3). Similarly, derivatisation reaction conditions have been chosen so as to give quantitative conversion of side-chain hydroxylated 3-oxo-4-ene oxysterols to their GP derivatives. Finally, the products of the derivatisation reaction were separated from unreacted starting material by solid phase extraction (SPE) on a C_{18} column and the methanol fractions subsequently analysed were those containing oxidised/derivatised oxysterols. Less polar sterols tailing into the Unisil fraction U2 (see supplementary Figure S2) similarly tail into a final methanol/chloroform fraction, which has not been analysed in detail by LC-MS^n.

Detailed Studies—The LTQ-Orbitrap provided data of considerably higher quality than that generated in the preliminary work using the LCQ ion-trap (above). The Orbitrap analyser was operated at 30,000 resolution, and gives mass accuracies of better than 5 ppm, allowing the confident prediction of elemental compositions of precursor ions ($[M]^+$)59. Further, by performing MS^n in the linear ion-trap (LIT) considerably higher sensitivity is achieved than is possible using the smaller cylindrical ion-trap of the LCQ. Additionally, the design of the LTQ-Orbitrap is such that while MS^n is performed in the LIT, the Orbitrap analyser can be used simultaneously to record the next mass spectrum at high resolution and mass accuracy, thereby allowing selection and elemental determination of subsequent precursor ions for MS^n in the LIT60.

Following oxidation/derivatisation monohydroxycholesterols give a molecular ion, $[M]^+$, at *m/z* 534.4054. In our preliminary study (above) it was difficult to differentiate 25- and 27-hydroxycholesterols from 24S-hydroxycholesterol. The improved chromatographic performance provided by the Hypersil Gold column packed with 1.9 μm particles allowed the separation of 24S-hydroxycholesterol (which as the GP derivative gives *syn* and *anti* conformers and appears as two peaks) from 25- and 27-hydroxycholesterols as seen by the RIC shown in Figure 2. Also evident in this Figure is a peak with retention time equivalent to that of 22R-hydroxycholesterol. The identification of these four oxysterols was confirmed by recording their MS^2 and MS^3 spectra and by comparing their retention times to authentic standards (see Figure 2 and Supplementary Figure S4). It is noticeable that the chromatographic pattern for the two regions of mouse CNS is similar. Additional monohydroxycholesterols were identified as 7α- and 7β-hydroxycholesterol (by comparison with reference standards), 6β-hydroxycholest-4-en-3-one and a compound giving a spectrum compatible to that expected from a hydroxylathosterol (no reference standard available, see supplementary Figure S4). 7α-Hydroxycholesterol can be formed enzymatically, while both 7-hydroxycholesterols isomers can be formed non-enzymatically by autoxidation. Further, 6β-hydroxycholest-4-en-3-one is formed as a side-product of the oxidation/derivatisation reactions of 5,6-epoxycholesterol which explains its high abundance (see Table 1 & 2). Quantitative estimates were made on the basis of peak areas in the RIC for the $[M]^+$ ion at *m/z* 534.4052 and assuming that the charge-tag gives a similar sensitivity for each oxysterol30 (Table 2).

It is a simple task to calculate the molecular formula and hence exact mass for all potential oxidised/derivatised oxysterols (and sterols). This was done over the range of cholestatrienol (*m/z* 514.3792) to trihydroxycholesterol (566.3952) including also oxosterols and their *bis* derivatives. Appropriate RICs were generated. By recording MS^2 and MS^3 spectra a number of further oxysterols were identified (Table 2). Shown in Figure 3 is the RIC for *m/z* 532.3898 corresponding to oxidised/derivatised oxocholesterols, epoxycholestenols and cholestadienediols. The MS^2 and MS^3 spectra of the first eluting component (6.63 min, Ctx) are *not* indicative of an oxoalcohol, and the MS^3 fragment ions at *m/z* 325, 353 and 367 (side-chain cleavage fragments ‘*e, ‘*f and ‘*g) indicate the additional functional group(s) are distal to C-24. The spectrum is identical to that of oxidised/derivatised 24S,25-epoxycholesterol (Figure 3b). By recording MS^2 and MS^3 spectra of the latter eluting peaks

in the chromatograms the mono-GP derivatives of oxidised 24-oxocholesterol (7.35 min, Ctx) and the mono GP derivative of 6-oxocholest-4-en-3-one (C^4-3,6-dione, 9.76 min, Ctx) were identified by comparison with reference standards. 6-Oxocholest-4-en-3-one is an autoxidation product of cholesterol30,61. Smith in his seminal book on cholesterol autoxidation describes the formation of this oxysterol by autoxidation of cholesterol via a 6-hydroperoxide (with $^1O_2$) and oxidation at C-3, or in our case it could be formed from the 3-oxo compound in the cholesterol oxidase reaction via a subsequent 6-hydroperoxide (with $^3O_2$)61. According to Smith there is no known enzymatic formation of the 3,6-dione.

Previous studies on adult rodent brain and cells from the CNS have identified the presence of dihydroxycholesterols30,32. Shown in Figure 4 are RIC for *m/z* 550.4003 corresponding to the $[M]^+$ ion of oxidised/derivatised dihydroxycholesterols in the cortex and spinal cord regions. Peaks eluting at 4.42 and 4.95 min (Ctx) correspond to 24,25-dihydroxycholesterol, presumably the *syn* and *anti* conformers of the derivative, while the peak eluting at 4.83 min (Ctx) also corresponds to a dihydroxycholesterol with the additional hydroxyl groups in the side-chain. The location of one hydroxyl group on C-24 is indicated by the MS^3 fragment-ion at *m/z* 353 (side-chain fragment '*f), while the reduced abundance of the MS^2 fragment-ion at *m/z* 453 ($[M-79-18]^+$) (cf. 24,25-dihydroxycholesterol) is indicative of the second additional hydroxyl group being located on C-27 giving 24,27-dihydroxycholesterol (see supplementary Figure S4). The MS^2 and MS^3 spectra of the late eluting dihydroxycholesterol (9.08 min, Ctx) suggest a cholestenetriol structure with three hydroxyl groups in the A/B rings or a dihydroxycholestanone with the additional hydroxyl and oxo group in the A/B rings. Earlier studies suggest that this is an autoxidation product of cholesterol30.

Epoxycholesterols are labile to the oxidation/derivatisation conditions employed in our study. As the derivatisation reaction proceeds in acidified 70% methanol, methanolysis can occur. This is evident for 24S,25-epoxycholesterol and leads to the formation of the 24-ol, 25-methylether (or 24-methylether,25-ol) in a reaction proceeding via a nucleophilic substitution-like mechanism62. The RICs for *m/z* 564.4160 from the cortex and spinal cord regions each gave peaks with retention times, MS^2 and MS^3 spectra equivalent to those derived from the 24S,25-epoxycholesterol standard (see Figure 5 and Figure S4). The occurrence of methanolysis suggests the possibility that hydrolysis of the epoxide may also have occurred. This would lead to the formation of the 24,25-diol, and it is thus likely that at least some of the identified 24,25-dihydroxycholesterol is derived from hydrolysis of the 24S,25-epoxide. The extent of epoxide hydrolysis has not been determined here, but this could be achieved by performing the oxidation/derivatisation reaction in acidified methanol/^{18}O-labelled water, but this was considered to be outside the scope of the present study.

The cholesterol 5,6-*seco*-sterol, 3β-hydroxy-5-oxo-5,6-*seco*cholestan-6-al, and its aldol, 3,5-dihydroxy-B-norcholestane-6-carboxyaldehyde have previously been found in brain and also the circulation (see supplementary Figure S1 for structures)30,41,44,63,64. Both molecules posses an oxo group (present prior to oxidation by cholesterol oxidase) which is reactive towards GP hydrazine and give an $[M]^+$ ion at *m/z* 552.4160. In both of the mouse CNS regions investigated in this study the presence of the aldol was evident having a retention time and giving an MS^2 spectrum identical to the authentic standard (see supplementary Figure S4).

Although MS^n spectra were recorded by data dependant analysis (DDA) with an include list, it was not possible to generate fragment-ion spectra of every eluting oxysterol, even upon replicate injections. Further, a number of oxysterol MS^n spectra were recorded which did not correspond to available standards, and were not readily interpretable. Table 2 lists all sterols

and oxysterols identified by their MS^n spectra and retention time from the CNS regions cortex and spinal cord and found in Unisil fraction U2 (oxysterol fraction). Also listed are partially identified compounds based on mass and isotopic pattern.

Using the Orbitrap mass spectrometer to record mass spectra at high resolution (30,000, full width at half maximum height, FWHM, definition) and generate exact mass RICs (± 5 ppm) it is possible to obtain quantitative information from peak areas. While the gold standard for quantitative studies is isotope dilution mass spectrometry it is necessary to first identify the potential analytes in a sample before the necessary isotope labelled standards are obtained. Oxysterol identification was the goal of the current study. However, the data obtained here is semi-quantitative. By assuming that oxidised/derivatised oxysterols give similar responses it is possible to estimate oxysterol amounts (Table 2). This is justified in the case of 3β-hydroxy-5-ene oxysterols which are structurally similar and should give similar ionisation efficiencies and yields upon oxidation/derivatisation. This is not necessarily so for other sterols and oxysterols.

In this study we have chosen to analyse unesterified sterols and oxysterols. This is on account of our interest in oxysterols as ligands to receptor proteins, i.e. LXR and INSIG, where binding requires the presence of a 3β-hydroxyl group on the ligand3,4,7. If interest were shifted to the total sterol and oxysterol content of brain, the lipid extract could be saponified25,48 and solvolysed25 prior to Unisil column chromatography. In our existing method designed to analyse unesterified sterols and oxysterols, oxysterols are separated from cholesterol and similarly hydrophobic sterols in an initial step by normal-phase chromatography (Unisil column), this minimises any contamination of the sample by autoxidation products of cholesterol which is present in >1000-fold excess. Clearly, any reactions performed prior to Unisil column chromatography may lead to autoxidation products of cholesterol which are not separated from endogenously formed oxysterols.

Discussion

In this study, we have profiled the sterol and oxysterol contents of the developing mouse CNS at E11, and identified a broad array of oxysterols in the cerebral cortex and spinal cord. Although the data is semi-quantitative, it provides a firm basis for future studies which can incorporate absolute quantitative measurements based on isotope labelled reference standards. The level of cholesterol, ~1 mg/g wet weight, is much lower than that found in adult mouse brain, ~20 mg/g20,55. However, the ratios of both desmosterol and lathosterol, two precursors of cholesterol, to cholesterol (both ~ 0.01) are greatly elevated when compared to the adult (0.001). This indicates that there is a high rate of cholesterol synthesis in CNS at this stage of development. On the other hand, the levels of oxysterols identified in E11 CNS are extremely low. 24S-Hydroxycholesterol, normally the most abundant oxysterol in brain21, is present at a level of ~ 20 ng/g at E11, this contrast with a concentration of 40 – 50 μg/g in adult mouse brain55. This data correlates with a recent report from Tint et al22 who studied the Dhcr7 knock out mouse. Tint et all suggest that it is only at E10 that the blood brain barrier begins to form, and only after this is the brain required to make essentially all its own sterols22. Prior to this the newly conceived mouse receives most of its sterols from its mother. This then explains the low cholesterol level in E11 mouse CNS and the high rate of synthesis at this time point. Further, Tint et al found low levels of CYP46A1 mRMA expression at E11.5 and that its expression starts to increase at E18-1922. This again agrees with our data where the 24S-hydroxycholesterol level was low at E11. Of some interest is the high level of 24S,25-epoxycholesterol in comparison to other oxysterols (24S,25-epoxycholesterol/24S-hydroxycholesterol > 5). Unlike other oxysterols which are metabolites of cholesterol, 24S,25-epoxycholesterol is formed via a shunt of the mevalonate pathway (Figure 1), and is not a metabolite of cholesterol but is

rather formed in parallel to it. An elevated level of 24S,25-epoxycholesterol could also be explained by an active mevalonate pathway. 24S,25-Epoxycholesterol has previously been identified in human brain cells and its rate of synthesis was found to be about 0.3% that of cholesterol in astrocytes and about 10-times lower in neurons38. By partially inhibiting 2,3-oxidosqualene cyclase (OSC) Wong et al were able to demonstrate an increase in 24S,25-epoxycholesterol synthesis in brain cells and modulation of the expression of genes regulated by the LXR and SREBP-238. As well as 24S-hydroxycholesterol and 24S,25-epoxycholesterol an array of other oxysterols were identified in mouse CNS including 7α-, 7β-, 22R-, 25-, and 27-hydroxycholesterol; and 24,25-, and 24,27-dihydroxycholesterol.

In summary, herein we report the first measurement of the oxysterol levels and their profile in the developing CNS. Our data show that, while hydroxycholesterols are expressed at low levels in both the cortex and spinal cord, 24S,25-epoxycholesterol, a putative LXR ligand, is present at relatively high levels. These results, together with the finding the LXR receptors are expressed in the developing brain10, suggest that 24S,25-epoxycholesterol may play a role during cortical and spinal cord development. Moreover, since the activity of LXR and their target genes have been linked to several diseases, such as Alzheimer's disease and motor neuron degeneration13, it would be of importance to examine the function of oxysterols also during brain development.

Methods

Animals

Sections of cortex and spinal cord from 25 - 30 E11 CD1 (Charles River Breeding Laboratories) embryonic mouse brains were manually dissected in sterile PBS saturated with argon and under argon flow in glass petri dishes, and subsequently prepared as described below. Mice were housed, bred, and treated according to the guidelines of the European Communities Council (directive 86/609/EEC) and the Society for Neuroscience (available at www.sfr.org/handbook). All experiments were approved by the local ethical committee (Stockholm Norra Djurförsöksetisks Nämnd number N154/06).

Sample Preparation

Sections of CNS were processed essentially as previously described by Griffiths and colleagues30,65. In brief, samples of CNS, 186 mg cortex and 119 mg spinal cord, collected under a stream of argon as above were extracted with ethanol (1 mL) and methylene chloride/methanol (1/1, v/v, 1 mL) containing butylhydroxytoluene (BHT), 10 μg/mL, and deaerated with a stream of argon. The extracts were taken to dryness and dissolved in methylene chloride/hexane (8:2, v/v, 2 mL) without BHT. This solution was applied to a silicic acid (Unisil) column (8 × 0.8 cm, 200 – 325 mesh in methylene chloride/hexane 8:2, v/v) followed by a wash with the same solvent (80 mL). The effluent was combined to give fraction U1. An oxysterol fraction was obtained by elution with ethyl acetate (10 mL) giving fraction U2 (see supplementary Figure S2).

After evaporation of solvents sterols/oxysterols were derivatised to TMS ethers47. These were analysed by GC-EI-MS. The GC-MS instrument consisted of a capillary GC (Hewlett Packard 5890, Avondale, PA, USA) connected to a single quadrupole mass spectrometer (Hewlett Packard, 5972) equipped with an EI source, operated at 70 eV. The MS was used in scan mode (*m/z* 50-700, 1 scan/sec). The injector was of cold on-column type and the capillary column was a fused-silica capillary column coated with cross-linked methyl silicone (25 m × 0.25 mm, 0.25-μm film thickness; J & W Scientific, Dalko Cromtech AB, Sollentuna, Sweden). The GC temperature program was as follows: 90 °C for 1 min, then 20

°C/min to 200 °C, then 5°C/min to 300 °C. Final temperature kept for 30 min. Quantitative estimates were made against a known amount of lathosterol TMS ether.

Following GC-MS analysis, the TMS ethers were hydrolysed with 0.1 M HCl in 80% aqueous methanol (1 hr at room temp) and the hydrolysate taken to dryness under nitrogen. Amounts of material corresponding to 150 mg cortex and 95 mg spinal cord were prepared for LC-MS/MS analysis. This was performed as outlined by Karu et al30. In brief, sterols were reconstituted in isopropanol (50 μL) and added to a solution of cholesterol oxidase (0.2 U from *Streptomyces sp*) in 1 ml of phosphate buffer (50 mM KH_2PO_4, pH 7). After 1 hr at 37 °C the reaction mixture was used as the starting solution for reaction with the Girard P (GP) hydrazine reagent (see supplementary Figure S3). After dilution with 2 mL of methanol, 150 mg of GP hydrazine and 150 μL of acetic acid were added and the mixture left at room temperature overnight. Oxidised/derivatised sterols from fraction U1 and oxysterols from fraction U2 were then separated from excess reagent by re-cycling solid phase extraction on a Sep-Pak C_{18} column (1 cm × 0.8 cm) as described by Karu et al30. GP derivatives were eluted in 2 mL of methanol. The most hydrophobic sterols were further eluted in a further 1mL of chloroform/methanol (1/1, v/v) (see supplementary Figure S2).

Capillary-LC-ES-MS^n

Preliminary experiments were performed by analysing the oxidised/derivatised oxysterols (and sterols) in fraction U2 by capillary-LC-ES-MS^n. On-line chromatographic separations were achieved utilising an Ultimate 3000 Capillary HPLC system (Dionex, Surrey, UK). ES-MS^n was performed on an LCQ ion-trap fitted with a nano-ES ion source (now Thermo Fisher, Hemel Hempstead, UK). 20 μL of the combined methanol eluate from the C_{18} SPE column (above) was diluted with 11.3 μL of 0.33% formic acid to give a 64% methanol solution containing 0.1% formic acid, and 4 μL (equivalent to ~ 120 (Sc) – 190 (Ctx) μg CNS) of the resultant solution injected onto a C_{18} capillary column (180 μm × 150 mm, 3 μm C_{18}, PepMap, Dionex). Oxidised/derivatised sterols and oxysterols were separated using a gradient program with a mobile phase A of 0.1% formic acid in 50% methanol and mobile phase B of 0.1% formic acid in 95% methanol. With a flow rate of 0.8 μL/min the mobile phase composition was raised from 30% B to 70% over the first 10 min, then to 80% B over the next 5 min, and maintained at 80% for a further 15 min, before returning to 30% B to recondition the column at 30% B for 20 min. Over this period MS, MS^2 and MS^3 spectra were recorded using a preset include list for the expected oxidised/derivatised sterols and oxysterols. For MS^n the isolation width was set at 2, the collision energy was 45%, three “microscans” were averaged, and the maximum injection time was 200 ms.

LC-ES-MS^n

Chromatographic separation of oxidised/derivatised oxysterols (and sterols) in fraction U2 was performed on a Finnigan Surveyor HPLC system utilising a Hypersil GOLD reversed-phase column (1.9 μm particles, 50 × 2.1 mm) from Thermo Fisher (San Jose, CA). Mobile phase A consisted of 50% methanol containing 0.1% formic acid, and mobile phase B consisted of 95% methanol containing 0.1% formic acid. After 1 min at 20% B, the proportion of B was raised to 80% B over the next 7 min, and maintained at 80% B for a further 5 min, before returning to 20% B in 6 s and re-equilibration for a further 3 min 54 s, giving a total run time of 17 min. The flow rate was maintained at 200 μL/min and eluent directed to the API source of an LTQ-Orbitrap mass spectrometer60.

Mass spectrometry analysis was performed on the LTQ-Orbitrap (Thermo Fisher, San Jose, CA) hybrid linear ion-trap (LIT) – Orbitrap analyser. Ions from the API source, operated in the positive ES mode, are initially stored in the LIT and analysed in either MS or MS^n modes. Ions can be detected at the LIT detector, or ejected axially and trapped in an

intermediate C-trap from which they are “squeezed” into the Orbitrap. Trapped ions in the Orbitrap assume circular trajectories around the central electrode and perform axial oscillation. The oscillating ions induce an image current into the two halves of the Orbitrap, which can be detected. The axial oscillation frequency of an ion (ω) is proportional to the square root of the inverse of *m/z*, $\{\omega = (k/m/z)^{1/2}\}$, and the frequencies of complex signals derived from many ions can be determined using a Fourier transformation (FT).

For the analysis of reference compounds (16 pg/μL) infused at 10 μL/min, the Orbitrap was operated at 60,000 resolution (FWHM definition). MS and MS^n spectra were recorded using both the LIT detector and the Orbitrap detector. The MS^2 isolation width was set at 2 so as to allow the selection of monoisotopic precursor ions. The Orbitrap was calibrated externally prior to each analytical session and mass accuracy was in all cases better than 5 ppm. For LC-MS and LC-MS^n analysis of reference compounds each sample (30 pg/μL in 60% methanol) was injected (10 μL) onto the reversed-phase column and eluted into the LTQ-Orbitrap at a flow-rate of 200 μL/min. The Orbitrap was operated at 30,000 resolution.

For the analysis of oxidised/derivatised sterols and oxysterols extracted from regions of embryonic CNS, 30 μL of the methanol eluent (2 mL) from the SPE C_{18} column (equivalent to ~ 1.43 (Sc) – 2.25 (Ctx) mg of CNS) was diluted with 20 μL of 0.25% formic acid and 20 μL aliquots injected onto the LC column (equivalent to ~ 0.57 (Sc) – 0.90 (Ctx) mg CNS). MS, MS^2 and MS^3 spectra were recorded in the DDA mode, with the incorporation of an inclusion list for expected oxidised/derivatised sterols and oxysterols (see supplementary Table S2). MS^3 was programmed to be performed on ions resulting from a neutral loss of 79 Da in the MS^2 scan. For the acquisition of MS^2 and MS^3 spectra the collision energy setting was 30 – 35.

Supplementary Material

Refer to Web version on PubMed Central for supplementary material.

Acknowledgments

This work was supported by the U.K. Biotechnology and Biological Sciences Research Council (BBSRC grant no. BB/C515771/1 and BB/C511356/1), the Swedish Research Council (VR), the STROKEMAP Project of the European Union (to EA), and Swansea University. We acknowledge Emmanuel Samuel for technical assistance.

References

1. McDonald JG, Thompson BM, McCrum EC, Russell DW. Extraction and analysis of sterols in biological matrices by high performance liquid chromatography electrospray ionization mass spectrometry. Methods Enzymol. 2007; 432:145–70. [PubMed: 17954216]
2. Janowski BA, Willy PJ, Devi TR, Falck JR, Mangelsdorf DJ. An oxysterol signalling pathway mediated by the nuclear receptor LXR alpha. Nature. Oct 24; 1996 383(6602):728–31. [PubMed: 8878485]
3. Janowski BA, Grogan MJ, Jones SA, Wisely GB, Kliewer SA, Corey EJ, Mangelsdorf DJ. Structural requirements of ligands for the oxysterol liver X receptors LXRalpha and LXRbeta. Proc Natl Acad Sci U S A. Jan 5; 1999 96(1):266–71. [PubMed: 9874807]
4. Lehmann JM, Kliewer SA, Moore LB, Smith-Oliver TA, Oliver BB, Su JL, Sundseth SS, Winegar DA, Blanchard DE, Spencer TA, Willson TM. Activation of the nuclear receptor LXR by oxysterols defines a new hormone response pathway. J Biol Chem. Feb 7; 1997 272(6):3137–40. [PubMed: 9013544]
5. Yang C, McDonald JG, Patel A, Zhang Y, Umetani M, Xu F, Westover EJ, Covey DF, Mangelsdorf DJ, Cohen JC, Hobbs HH. Sterol intermediates from cholesterol biosynthetic pathway as liver X receptor ligands. J Biol Chem. Sep 22; 2006 281(38):27816–26. [PubMed: 16857673]

6. Goldstein JL, DeBose-Boyd RA, Brown MS. Protein sensors for membrane sterols. Cell. Jan 13; 2006 124(1):35–46. [PubMed: 16413480]
7. Radhakrishnan A, Ikeda Y, Kwon HJ, Brown MS, Goldstein JL. Sterol-regulated transport of SREBPs from endoplasmic reticulum to Golgi: oxysterols block transport by binding to Insig. Proc Natl Acad Sci U S A. Apr 17; 2007 104(16):6511–8. [PubMed: 17428920]
8. Millatt LJ, Bocher V, Fruchart JC, Staels B. Liver X receptors and the control of cholesterol homeostasis: potential therapeutic targets for the treatment of atherosclerosis. Biochim Biophys Acta. Mar 17; 2003 1631(2):107–18. [PubMed: 12633677]
9. Kainu T, Kononen J, Enmark E, Gustafsson JA, Pelto-Huikko M. Localization and ontogeny of the orphan receptor OR-1 in the rat brain. J Mol Neurosci. Spring;1996 7(1):29–39. [PubMed: 8835780]
10. Annicotte JS, Schoonjans K, Auwerx J. Expression of the liver X receptor alpha and beta in embryonic and adult mice. Anat Rec A Discov Mol Cell Evol Biol. Apr; 2004 277(2):312–6. [PubMed: 15052659]
11. Wang L, Schuster GU, Hultenby K, Zhang Q, Andersson S, Gustafsson JA. Liver X receptors in the central nervous system: from lipid homeostasis to neuronal degeneration. Proc Natl Acad Sci U S A. Oct 15; 2002 99(21):13878–83. Epub 2002 Oct 4. Erratum in: Proc Natl Acad Sci U S A. 2006 May 23;103(21):8298. [PubMed: 12368482]
12. Andersson S, Gustafsson N, Warner M, Gustafsson JA. Inactivation of liver X receptor beta leads to adult-onset motor neuron degeneration in male mice. Proc Natl Acad Sci U S A. Mar 8; 2005 102(10):3857–62. Epub 2005 Feb 28. Erratum in: Proc Natl Acad Sci U S A. 2006 May 23;103(21):8298. [PubMed: 15738425]
13. Kim HJ, Fan X, Gabbi C, Yakimchuk K, Parini P, Warner M, Gustafsson JA. Liver X receptor beta (LXRbeta): a link between beta-sitosterol and amyotrophic lateral sclerosis-Parkinson's dementia. Proc Natl Acad Sci U S A. Feb 12; 2008 105(6):2094–9. [PubMed: 18238900]
14. Horton JD, Goldstein JL, Brown MS. SREBPs: activators of the complete program of cholesterol and fatty acid synthesis in the liver. J Clin Invest. May; 2002 109(9):1125–31. [PubMed: 11994399]
15. Radhakrishnan A, Sun LP, Kwon HJ, Brown MS, Goldstein JL. Direct binding of cholesterol to the purified membrane region of SCAP: mechanism for a sterol-sensing domain. Mol Cell. Jul 23; 2004 15(2):259–68. [PubMed: 15260976]
16. Sun LP, Li L, Goldstein JL, Brown MS. Insig required for sterol-mediated inhibition of Scap/SREBP binding to COPII proteins in vitro. J Biol Chem. Jul 15; 2005 280(28):26483–90. [PubMed: 15899885]
17. Adams CM, Reitz J, De Brabander JK, Feramisco JD, Li L, Brown MS, Goldstein JL. Cholesterol and 25-hydroxycholesterol inhibit activation of SREBPs by different mechanisms, both involving SCAP and Insigs. J Biol Chem. Dec 10; 2004 279(50):52772–80. [PubMed: 15452130]
18. Sever N, Yang T, Brown MS, Goldstein JL, DeBose-Boyd RA. Accelerated degradation of HMG CoA reductase mediated by binding of insig-1 to its sterol-sensing domain. Mol Cell. Jan; 2003 11(1):25–33. [PubMed: 12535518]
19. Song BL, Javitt NB, DeBose-Boyd RA. Insig-mediated degradation of HMG CoA reductase stimulated by lanosterol, an intermediate in the synthesis of cholesterol. Cell Metab. Mar; 2005 1(3):179–89. [PubMed: 16054061]
20. Dietschy JM, Turley SD. Thematic review series: brain Lipids. Cholesterol metabolism in the central nervous system during early development and in the mature animal. J Lipid Res. Aug; 2004 45(8):1375–97. [PubMed: 15254070]
21. Björkhem I, Lütjohann D, Breuer O, Sakinis A, Wennmalm A. Importance of a novel oxidative mechanism for elimination of brain cholesterol. Turnover of cholesterol and 24(S)-hydroxycholesterol in rat brain as measured with 18O2 techniques in vivo and in vitro. J Biol Chem. Nov 28; 1997 272(48):30178–84. [PubMed: 9374499]
22. Tint GS, Yu H, Shang Q, Xu G, Patel SB. The use of the Dhcr7 knockout mouse to accurately determine the origin of fetal sterols. J Lipid Res. Jul; 2006 47(7):1535–41. [PubMed: 16651660]

23. Heverin M, Meaney S, Lütjohann D, Diczfalusy U, Wahren J, Björkhem I. Crossing the barrier: net flux of 27-hydroxycholesterol into the human brain. J Lipid Res. May; 2005 46(5):1047–52. [PubMed: 15741649]
24. Lund EG, Guileyardo JM, Russell DW. cDNA cloning of cholesterol 24-hydroxylase, a mediator of cholesterol homeostasis in the brain. Proc Natl Acad Sci U S A. Jun 22; 1999 96(13):7238–43. [PubMed: 10377398]
25. Lütjohann D, Björkhem I, Locatelli S, Dame C, Schmolling J, von Bergmann K, Fahnenstich H. Cholesterol dynamics in the foetal and neonatal brain as reflected by circulatory levels of 24S-hydroxycholesterol. Acta Paediatr. Jun; 2001 90(6):652–7. [PubMed: 11440099]
26. Ohyama Y, Meaney S, Heverin M, Ekström L, Brafman A, Shafir M, Andersson U, Olin M, Eggertsen G, Diczfalusy U, Feinstein E, Björkhem I. Studies on the transcriptional regulation of cholesterol 24-hydroxylase (CYP46A1): marked insensitivity toward different regulatory axes. J Biol Chem. Feb 17; 2006 281(7):3810–20. [PubMed: 16321981]
27. Quan G, Xie C, Dietschy JM, Turley SD. Ontogenesis and regulation of cholesterol metabolism in the central nervous system of the mouse. Brain Res Dev Brain Res. Dec 19; 2003 146(1-2):87–98.
28. Lin YY, Welch M, Lieberman S. The detection of 20S-hydroxycholesterol in extracts of rat brains and human placenta by a gas chromatograph/mass spectrometry technique. J Steroid Biochem Mol Biol. May; 2003 85(1):57–61. [PubMed: 12798357]
29. Yao ZX, Brown RC, Teper G, Greeson J, Papadopoulos V. 22R-Hydroxycholesterol protects neuronal cells from beta-amyloid-induced cytotoxicity by binding to beta-amyloid peptide. J Neurochem. Dec; 2002 83(5):1110–9. [PubMed: 12437582]
30. Karu K, Hornshaw M, Woffendin G, Bodin K, Hamberg M, Alvelius G, Sjövall J, Turton J, Wang Y, Griffiths WJ. Liquid chromatography-mass spectrometry utilizing multi-stage fragmentation for the identification of oxysterols. J Lipid Res. Apr; 2007 48(4):976–87. [PubMed: 17251593]
31. Mast N, Norcross R, Andersson U, Shou M, Nakayama K, Bjorkhem I, Pikuleva IA. Broad substrate specificity of human cytochrome P450 46A1 which initiates cholesterol degradation in the brain. Biochemistry. Dec 9; 2003 42(48):14284–92. [PubMed: 14640697]
32. Zhang J, Akwa Y, el-Etr M, Baulieu EE, Sjövall J. Metabolism of 27-, 25- and 24-hydroxycholesterol in rat glial cells and neurons. Biochem J. Feb 15; 1997 322(Pt 1):175–84. [PubMed: 9078259]
33. Rose K, Allan A, Gauldie S, Stapleton G, Dobbie L, Dott K, Martin C, Wang L, Hedlund E, Seckl JR, Gustafsson JA, Lathe R. Neurosteroid hydroxylase CYP7B: vivid reporter activity in dentate gyrus of gene-targeted mice and abolition of a widespread pathway of steroid and oxysterol hydroxylation. J Biol Chem. Jun 29; 2001 276(26):23937–44. [PubMed: 11290741]
34. Jelinek DF, Andersson S, Slaughter CA, Russell DW. Cloning and regulation of cholesterol 7 alpha-hydroxylase, the rate-limiting enzyme in bile acid biosynthesis. J Biol Chem. May 15; 1990 265(14):8190–7. [PubMed: 2335522]
35. Mellon SH, Griffin LD. Neurosteroids: biochemistry and clinical significance. Trends Endocrinol Metab. Jan-Feb;2002 13(1):35–43. [PubMed: 11750861]
36. Eneroth P, Gustafsson J. Steroids in newborns and infants. Hydroxylated cholesterol derivatives in the steroid monosulphate fraction from meconium. FEBS Lett. Apr; 1969 3(2):129–132. [PubMed: 11946987]
37. Nelson JA, Steckbeck SR, Spencer TA. Biosynthesis of 24,25-epoxycholesterol from squalene 2,3;22,23-dioxide. J Biol Chem. Feb 10; 1981 256(3):1067–8. [PubMed: 7451488]
38. Wong J, Quinn CM, Guillemin G, Brown AJ. Primary human astrocytes produce 24(S),25-epoxycholesterol with implications for brain cholesterol homeostasis. J Neurochem. Dec; 2007 103(5):1764–73. [PubMed: 17956548]
39. Wong J, Quinn CM, Gelissen IC, Brown AJ. Endogenous 24(S),25-epoxycholesterol fine-tunes acute control of cellular cholesterol homeostasis. J Biol Chem. Jan 11; 2008 283(2):700–7. [PubMed: 17981807]
40. Wang, Y.; Griffiths, WJ. Steroids, Sterols and the Nervous System. In: Griffiths, WJ., editor. Metabolomics, Metabonomics and Metabolite Profiling. Cambridge, UK: 2008. RSC Biomolecular Sciences Series

41. Griffiths WJ, Hornshaw M, Woffendin G, Baker SF, Lockhart A, Heidelberger S, Gustafsson M, Sjövall J, Wang Y. Discovering Oxysterols in Plasma: A Window on the Metabolome. J Proteome Res. Aug 1; 2008 7(8):3602–3612. [PubMed: 18605750]
42. Axelson M, Sjövall J. Potential bile acid precursors in plasma--possible indicators of biosynthetic pathways to cholic and chenodeoxycholic acids in man. J Steroid Biochem. Aug 28; 1990 36(6): 631–40. [PubMed: 2214780]
43. Schroepfer GJ Jr. Oxysterols: modulators of cholesterol metabolism and other processes. Physiol Rev. Jan; 2000 80(1):361–554. [PubMed: 10617772]
44. Wentworth P Jr, Nieva J, Takeuchi C, Galve R, Wentworth AD, Dilley RB, DeLaria GA, Saven A, Babior BM, Janda KD, Eschenmoser A, Lerner RA. Evidence for ozone formation in human atherosclerotic arteries. Science. Nov 7; 2003 302(5647):1053–6. [PubMed: 14605372]
45. Rosen H, Reshef A, Maeda N, Lippoldt A, Shpizen S, Triger L, Eggertsen G, Björkhem I, Leitersdorf E. Markedly reduced bile acid synthesis but maintained levels of cholesterol and vitamin D metabolites in mice with disrupted sterol 27-hydroxylase gene. J Biol Chem. Jun 12; 1998 273(24):14805–12. [PubMed: 9614081]
46. Li-Hawkins J, Lund EG, Turley SD, Russell DW. Disruption of the oxysterol 7alpha-hydroxylase gene in mice. J Biol Chem. Jun 2; 2000 275(22):16536–42. [PubMed: 10748048]
47. Griffiths, W.; Shackleton, CHL.; Sjovall, J. Steroid Analysis. In: Caprioli, R., editor. The Encyclopedia of Mass Spectrometry. Vol. 3. Elsevier; Amsterdam: 2005. p. 447-473.
48. Dzeletovic S, Breuer O, Lund E, Diczfalusy U. Determination of cholesterol oxidation products in human plasma by isotope dilution-mass spectrometry. Anal Biochem. Feb 10; 1995 225(1):73–80. [PubMed: 7778789]
49. Babiker A, Diczfalusy U. Transport of side-chain oxidized oxysterols in the human circulation. Biochim Biophys Acta. Jun 15; 1998 1392(2-3):333–9. [PubMed: 9630709]
50. Wang Y, Karu K, Griffiths WJ. Analysis of neurosterols and neurosteroids by mass spectrometry. Biochimie. Feb; 2007 89(2):182–91. [PubMed: 17126470]
51. Wang Y, Griffiths WJ. Capillary liquid chromatography combined with tandem mass spectrometry for the study of neurosteroids and oxysterols in brain. Neurochem Int. Mar-Apr;2008 52(4-5):506–21. [PubMed: 17850923]
52. Burkard I, Rentsch KM, von Eckardstein A. Determination of 24S- and 27-hydroxycholesterol in plasma by high-performance liquid chromatography-mass spectrometry. J Lipid Res. Apr; 2004 45(4):776–81. [PubMed: 14729854]
53. Debarber AE, Lütjohann D, Merkens L, Steiner RD. Liquid chromatography-tandem mass spectrometry determination of plasma 24S-hydroxycholesterol with chromatographic separation of 25-hydroxycholesterol. Anal Biochem. Jun 12.2008
54. Jiang X, Ory DS, Han X. Characterization of oxysterols by electrospray ionization tandem mass spectrometry after one-step derivatization with dimethylglycine. Rapid Commun Mass Spectrom. 2007; 21(2):141–52. [PubMed: 17154356]
55. Lütjohann D, Brzezinka A, Barth E, Abramowski D, Staufenbiel M, von Bergmann K, Beyreuther K, Multhaup G, Bayer TA. Profile of cholesterol-related sterols in aged amyloid precursor protein transgenic mouse brain. J Lipid Res. Jul; 2002 43(7):1078–85. [PubMed: 12091492]
56. Björkhem I, Miettinen T, Reihnér E, Ewerth S, Angelin B, Einarsson K. Correlation between serum levels of some cholesterol precursors and activity of HMG-CoA reductase in human liver. J Lipid Res. Oct; 1987 28(10):1137–43. [PubMed: 3681138]
57. Banner CD. Sources of plant sterol contaminants encountered in low level steroid analysis. J Chromatogr. Dec 6; 1991 572(1-2):307–11. [PubMed: 1818065]
58. MacLachlan J, Wotherspoon AT, Ansell RO, Brooks CJ. Cholesterol oxidase: sources, physical properties and analytical applications. J Steroid Biochem Mol Biol. Apr; 2000 72(5):169–95. [PubMed: 10822008]
59. Beynon JH. Qualitative analysis of organic compounds by mass spectrometry. Nature. 1954; 174:735.
60. Makarov A, Denisov E, Kholomeev A, Balschun W, Lange O, Strupat K, Horning S. Performance evaluation of a hybrid linear ion trap/orbitrap mass spectrometer. Anal Chem. Apr 1; 2006 78(7): 2113–20. [PubMed: 16579588]

61. LL Smith Cholesterol autoxidation. Plenum Press; New York and London: 1981.
62. Griffiths WJ, Wang Y. Eur J Lipid Sci Technol. 2008 in press.
63. Zhang Q, Powers ET, Nieva J, Huff ME, Dendle MA, Bieschke J, Glabe CG, Eschenmoser A, Wentworth P Jr, Lerner RA, Kelly JW. Metabolite-initiated protein misfolding may trigger Alzheimer's disease. Proc Natl Acad Sci U S A. Apr 6; 2004 101(14):4752–7. [PubMed: 15034169]
64. Bieschke J, Zhang Q, Bosco DA, Lerner RA, Powers ET, Wentworth P Jr, Kelly JW. Small molecule oxidation products trigger disease-associated protein misfolding. Acc Chem Res. Sep; 2006 39(9):611–9. [PubMed: 16981677]
65. Griffiths WJ, Wang Y, Alvelius G, Liu S, Bodin K, Sjövall J. Analysis of oxysterols by electrospray tandem mass spectrometry. J Am Soc Mass Spectrom. Mar; 2006 17(3):341–62. [PubMed: 16442307]

Europe PMC Funders Author Manuscripts

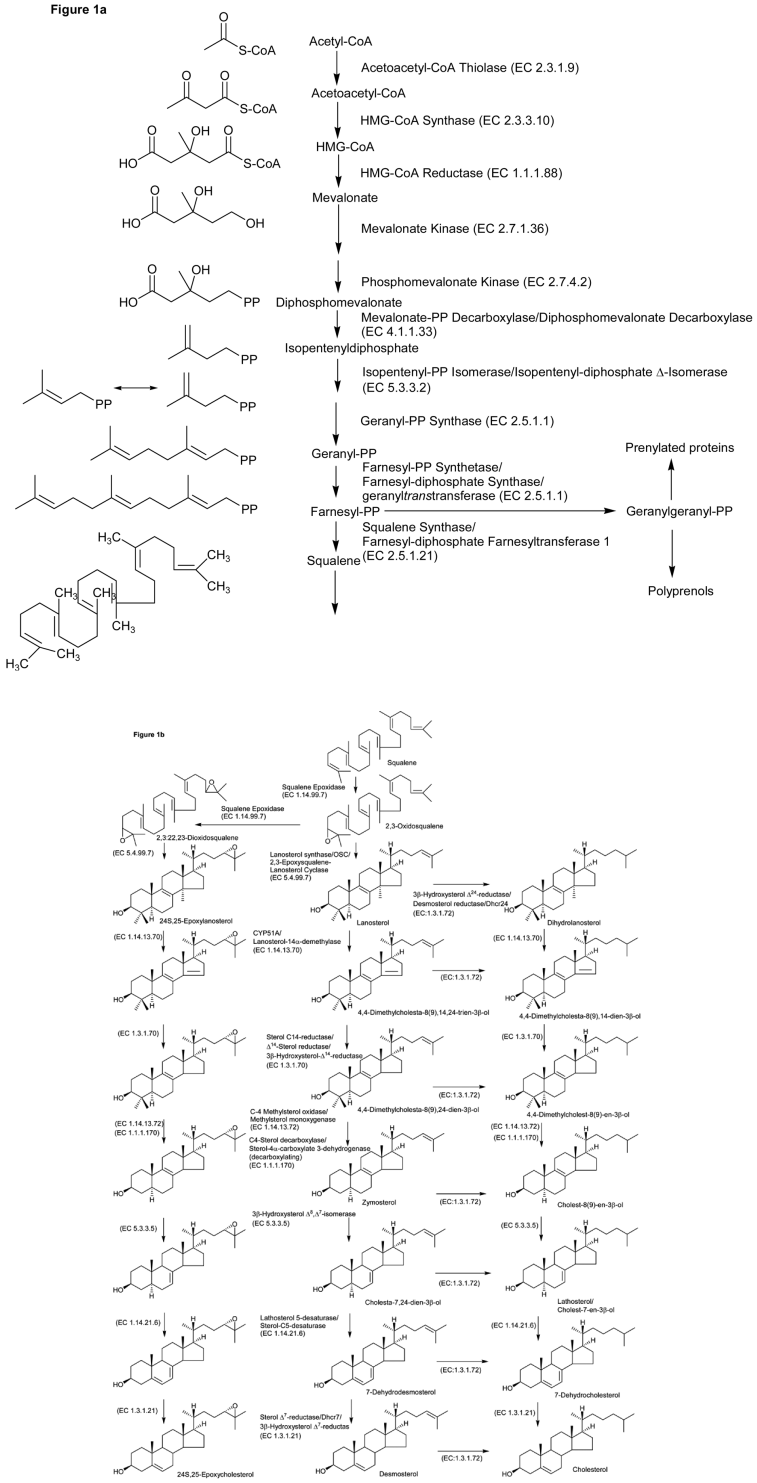

Figure 1.
Overview of the cholesterol and 24S,25-epoxycholesterol synthetic pathways.

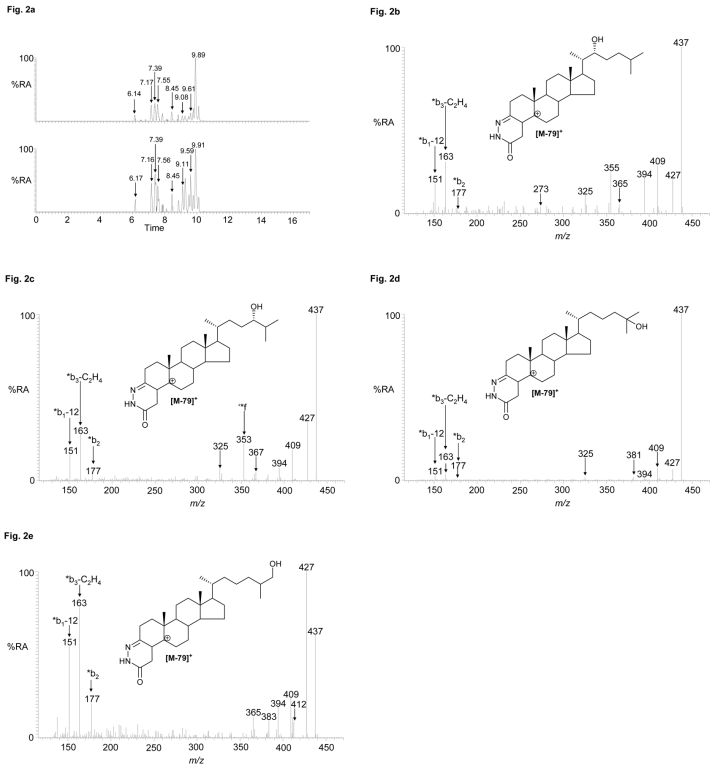

Figure 2.

(a) RICs for oxidised/derivatised monohydroxycholesterol $[M]^+$ ions, *m/z* 534.4054, from data generated by the LTQ-Orbitrap (*m/z* window ± 5 ppm). The upper trace is from cortex (magnified by a factor of 15 over the range 6 – 9 min), and the lower trace from spinal cord (magnified by a factor of 10 over the range 6 – 9 min). Chromatographic conditions are described in the Experimental. Spectra were recorded using the Orbitrap mass analyser. See Table 2 for the identification of chromatographic peaks. **(b-d)** MS^3 (534→455→) spectra of chromatographic peaks eluting at **(b)** 6.14 min (22R-hydroxycholesterol), **(c)** 7.17 min (24S-hydroxycholesterol), **(d)** 7.39 min (25-hydroxycholesterol), and **(e)** 8.45 min (27-hydroxycholesterol) from the cortex region. MS^3 spectra were recorded using the LTQ detector. Shown in supplementary Figure S4 are spectra of other oxysterols identified in brain sections and where applicable spectra of authentic standards. The LC-MS^n method is illustrated in supplementary Figure S5.

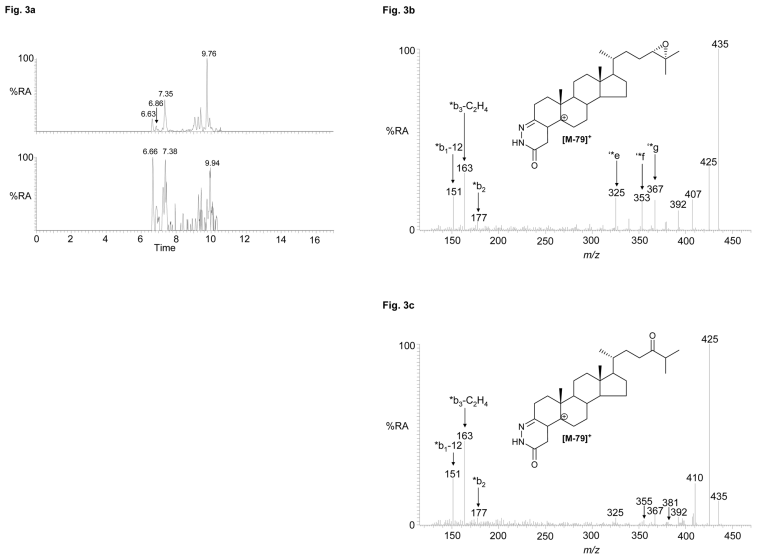

Figure 3

. **(a)** RICs for oxidised/derivatised oxysterol $[M]^+$ ions, *m/z* 532.3898, from CNS regions cortex (upper trace) and spinal cord (lower trace). **(b & c)** MS^3 (532→453→) spectra of chromatographic peaks eluting at **(b)** 6.63 min (24S,25-epoxycholesterol), and (**c**) 7.35 min (24-oxocholesterol) from the cortex sample. Data was acquired on the LTQ-Orbitrap. RIC (± 5 ppm) were generated using the Orbitrap detector, and MS^3 spectra were recorded using the LTQ detector. Chromatographic conditions are described in the Experimental. Shown in supplementary Figure S4 are spectra of other oxysterols identified and where applicable spectra of authentic standards.

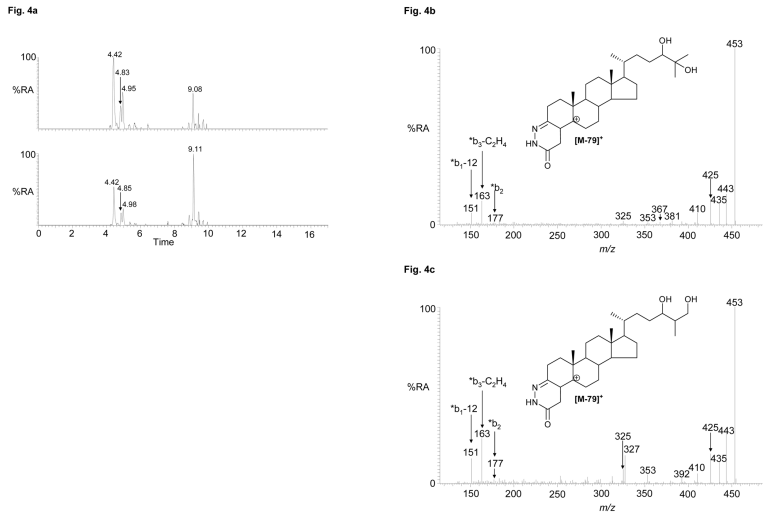

Figure 4.

(a) RICs for oxidised/derivatised oxysterol $[M]^+$ ions, *m/z* 550.4003, from cortex (upper trace) and spinal cord (lower trace). **(b & c)** MS^3 (550→471→) spectra of chromatographic peaks eluting at **(b)** 4.42 min (24,25-dihydroxycholesterol), and (**c**) 4.83 min (24,27-dihydroxycholesterol) from the cortex sample. Data was acquired on the LTQ-Orbitrap. RICs (± 5 ppm) were generated using the Orbitrap detector, and MS^3 spectra were recorded using the LTQ detector. Chromatographic conditions are described in the Experimental. Shown in supplementary Figure S4 are spectra of other oxysterols identified and where applicable spectra of authentic standards.

Europe PMC Funders Author Manuscripts

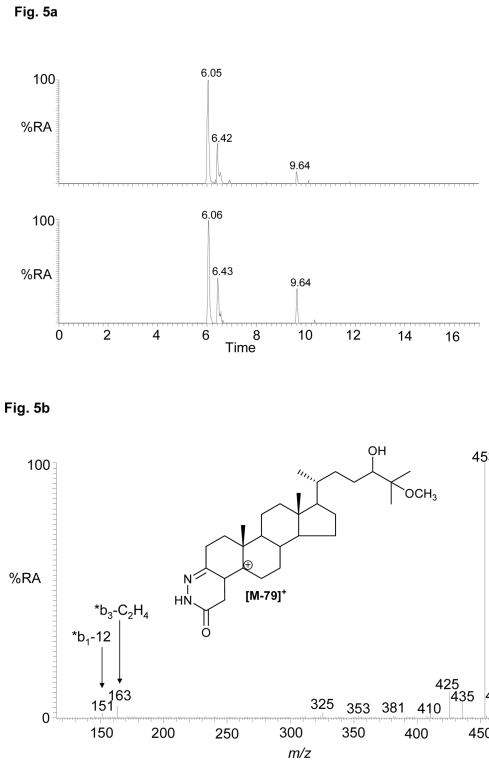

Figure 5.

(a) RICs for oxidised/derivatised oxysterol $[M]^+$ ions, *m/z* 564.4160 from the cortex (upper trace) and spinal cord (lower trace) regions of CNS. **(b)** MS^3 (564→485→) spectrum of the chromatographic peak eluting at 6.05 min (24-hydroxy,25-methoxycholesterol or 24-methoxy,25-hydroxycholesterol) from the cortex. Data was acquired on the LTQ-Orbitrap. RICs (± 5 ppm) were generated using the Orbitrap detector, and the MS^3 spectrum was recorded using the LTQ detector. Chromatographic conditions are described in the Experimental. Shown in supplementary Figure S4 are spectra of other oxysterols and where applicable spectra of authentic standards.

Europe PMC Funders Author Manuscripts

Table 1

GC-MS analyses of unesterified sterols in cortex and spinal cord of mice. M^+ and RI are for the analysed TMS ether derivatives.

Trivial name	Abbreviation[a]	M^+	RI	Concentration (μg/g)[b]		Comment
		m/z	(Kovats)	Cortex	Spinal cord	
Cholesterol	C^5-3β-ol	458	3150	1250	1150	
Desmosterol	$C^{5,24}$-3β-ol	456	3168	37.5	17	
Lathosterol	C^7-3β-ol	458	3188	14	13.8	
Zymosterol	5α-$C^{8(9),24}$-3β-ol	456	3220	3	2.1	Or Δ^{24}-lathosterol, no reference
5β,6β-Epoxycholesterol	C-3β-ol-5β,6β-epoxide	474	3245	0.8	1.8	Autoxidation product
Campesterol	24-Me-C^5-3β-ol	472	3249	6.5	4.2	Contaminant
5α,6α-Epoxycholesterol	C-3β-ol-5α,6α-epoxide	474	3260	1.2	3	Autoxidation product
Cholestenediol	C^5-3,x-diol	546	3261	ND	15.6	No reference
Cholestanediol	C-3,x-diol	548	3265	1.1	1.2	No reference
Lanosterol	4,4,14-Me_3-5α-$C^{8(9),24}$-3β-ol	498	3319	3.3	2.3	Contaminant
Sitosterol	24-Et-C^5-3β-ol	486	3345	2	1.6	Contaminant

ND not detected

[a] C=cholestane; superscript=position of double bond; greek letter=orientation of hydroxyl group.

[b] Quantitative estimates

Europe PMC Funders Author Manuscripts

Table 2

Unesterified Oxysterol Content of Foetal CNS Regions Cortex (Ctx) and Spinal Cord (Sc) as Determined by LC-MS^n using the LTQ-Orbitrap

		Ctx[a]		Sc[a]				
Identified Structure after Treatment with Cholesterol Oxidase	**[M]$^+$ of GP *m/z***	**μg/g**	**Rt/min**	**μg/g**	**Rt/min**	**Inferred Structure prior to Treatment with Cholesterol Oxidase**	**Inferred Compound Trivial Name**	**Comment/ Parameters for Identification**
C-4,24-diene-3-one	516.3948	NM	10.53	NM	10.52	C-5,24-diene-3β-ol	Desmosterol	Rt, MS^n
C-4,7(or8)-diene-3-one	516.3948	NM	11.00	ND		C-5,7(or 8)-diene-3β-ol	7(or 8)-Dehydrocholesterol[b]	Rt, MS^n
C-4-ene-3-one	518.4105	NM	11.43	NM	11.43	C-5-ene-3β-ol	Cholesterol	Rt, MS^n
24-Me-C-4-ene-3-one	532.4261	NM	12.13	NM	12.09	24-Me-C-5-ene-3β-ol	Campesterol	Contaminant[c], MS^n
24-Et-C-4-ene-3-one	546.4418	NM	12.84	NM	12.76	24-Et-C-5-ene-3β-ol	Sitosterol	Contaminant[c], MS only[d]
C-X,Y,Z-triene-x-ol-y-one	530.3741	0.008	9.10	ND		C-X,Y,Z-triene-3β,x-diol[e]	Unknown[e]	MS only[d]
C-4-ene-24S,25-epoxide-3-one	532.3898	0.043	6.63/6.86	0.022	6.66/6.85	C-5-ene-3β-ol-24S,25-epoxide	24S,25-Epoxycholesterol	Appear as *syn* and *anti* conformers, Rt, MS^n
C-4-ene-24-ol,25-OMe-3-one[f]	564.4160	0.122	6.05/6.42	0.069	6.06/6.43	C-5-ene-3β-ol-24S,25-epoxide	24S,25-Epoxycholesterol	Appear as *syn* and *anti* conformers, Rt, MS^n
		0.165		**0.091**		**C-5-ene-3β-ol-24S,25-epoxide**	**24S,25-Epoxycholesterol**	**Total 24S,25-Epoxycholesterol**
C-4-ene-3,24-dione	532.3898	0.093	7.35	0.013	7.38	C-5-ene-3β-ol-24-one	24-Oxocholesterol	Rt, MS^n
C-4-ene-3,6-dione	532.3898	0.185	9.76	0.019	9.94	C-4-ene-3,6-dione[g]	6-Oxocholestenone[g]	Autoxidation, Rt, MS^n
C-4-ene-22R-ol-3-one	534.4054	0.004	6.14	0.002	6.17	C-5-ene-3β,22R-diol	22R-Hydroxycholesterol	Rt, MS^n
C-4-ene-24S-ol-3-one	534.4054	0.026	7.17/7.55	0.013	7.16/7.56	C-5-ene-3β,24S-diol	24S-Hydroxycholesterol	Appear as *syn* and *anti* conformers, Rt, MS^n
C-4-ene-25-ol-3-one	534.4054	0.016	7.39	0.012	7.39	C-5-ene-3β,25-diol	25-Hydroxycholesterol	Rt, MS^n
C-4-ene-27-ol-3-one	534.4054	0.011	8.45/8.83	0.006	8.45/8.85	C-5-ene-3β,27-diol	27-Hydroxycholesterol	Appear as *syn* and *anti* conformers, Rt, MS^n
C-4-ene-7β-ol-3-one	534.4054	0.052	9.08/9.48	0.053	9.11/9.5	C-5-ene-3β,7β-diol	7β-Hydroxycholesterol	Autoxidation, appears

Identified Structure after Treatment with Cholesterol Oxidase	[M]+ of GP m/z	Ctx[a] µg/g	Ctx[a] Rt/min	Sc[a] µg/g	Sc[a] Rt/min	Inferred Structure prior to Treatment with Cholesterol Oxidase	Inferred Compound Trivial Name	Comment/ Parameters for Identification
C-4-ene-7α-ol-3-one	534.4054	0.055	9.61	0.067	9.59	C-5-ene-3β,7α-diol	7α-Hydroxycholesterol[h]	Rt, MS[n]
C-7-ene-x-ol-3-one	534.4054	0.152	9.27/9.78	0.103	9.26/9.76	C-7-ene-3β,x-diol	Hydroxylathosterol	No reference, MS[n]
C-4-ene-6β-ol-3-one	534.4054	0.568	9.89	0.109	9.89	C-4-ene-6β-ol-3-one/C-3β,5α,6β-triol/C-3β-ol-5,6-epoxide[i]	6β-hydroxycholest-4-en-3-one/cholestane-3β,5α,6β-triol/5,6-epoxycholesterol[i]	Autoxidation, Rt, MS[n]
C-X,Y,Z-triene-x,y-diol-z-one	546.369	0.009	8.34	ND		C-X,Y,Z-triene-3β,x,y-triol[j]	Unknown[j]	MS-only[d]
C-X,Y,Z-triene-x,y-diol-z-one	546.369	0.009	8.7	0.002	8.71	C-X,Y,Z-triene-3β,x,y-triol[j]	Unknown[j]	MS-only[d]
C-X,Y,Z-triene-x,y-diol-z-one	546.369	0.026	9.29	ND		C-X,Y,Z-triene-3β,x,y-triol[j]	Unknown[j]	MS-only[d]
C-X,Y-diene-x,y-diol-z-one	548.3847	0.004	5.45	ND		C-X,Y-diene-3β,x,y-triol[k]	Unknown[k]	MS[n]
C-X,Y-diene-x,y-diol-z-one	548.3847	ND		0.001	7.31	C-X,Y-diene-3β,x,y-triol[k]	Unknown[k]	MS-only[d]
C-X,Y-diene-x,y-diol-z-one	548.3847	0.028	9.78	0.007	9.76	C-X,Y-diene-3β,x,y-triol[k]	Unknown[k]	MS[n]
C-X,Y-diene-x,y-diol-z-one	548.3847	0.009	10.05	0.002	10.07	C-X,Y-diene-3β,x,y-triol[k]	Unknown[k]	MS[n]
C-4-ene-24,25-diol-3-one	550.4003	0.070	4.42/4.95	0.038	4.42/4.98	C-5-ene-3β,24,25-triol	24,25-Dihydroxycholesterol	Appear as *syn* and *anti* conformers, Rt, MS[n]
C-4-ene-24,27-diol-3-one	550.4003	0.007	4.83	0.006	4.85	C-5-ene-3β,24,27-triol	24,27-Dihydroxycholesterol	No reference, MS[n]
C-x-ol-y,z-dione	550.4003	0.017	9.08	0.041	9.11	C-3β,x-diol-y-one[L]	Unknown[L]	MS[n]
C-x,y-diol-z-one	552.4160	0.002	5.67	0.001	5.68	C-3β,x,y-triol	Unknown	MS-only[d]
C-x,y-diol-z-one	552.4160	0.018	9.44/9.89	0.002	9.47	C-3β,x,y-triol	Unknown	appears as *syn* and *anti* conformers, MS[n]

Europe PMC Funders Author Manuscripts

		Ctx[a]		Sc[a]				
Identified Structure after Treatment with Cholesterol Oxidase	**$[M]^+$ of GP *m/z***	**μg/g**	**Rt/min**	**μg/g**	**Rt/min**	**Inferred Structure prior to Treatment with Cholesterol Oxidase**	**Inferred Compound Trivial Name**	**Comment/ Parameters for Identification**
Aldol	552.4160	0.066	9.59	0.075	9.59	aldol[m]	aldol[m]	MS^n

C = cholestane; NM = not measured; Rt = retention time; ND = not detected; No reference = no authentic standard available

[a]Data for GP derivatives. Quantitative estimates based on replicate analysis

[b]7- and 8-dehyrocholesterol are not resolved

[c]Possibly a contaminant

[d]Identification based on exact mass and isotopic pattern only

[e]Alternatively C-X,Y-dien-3β-ol-x-one

[f]Alternatively C-4-ene-25-ol,24-OMe-3-one, methanolysis product of C-4-ene-24S,25-epoxide-3-one

[g]C-4-ene-3,6-dione reacts with GP reagent without oxidation by cholesterol oxidase

[h]Formed enzymatically by CYP7A1 and/or by autoxidation

[i]C-4-ene-6β-ol-3-one can be formed from C-3β,5α,6β-triol and C-3β-ol-5,6-epoxides during the cholesterol oxidase/GP derivatisation reaction

[j]Alternatively C-X,Y-diene-3β,x-diol-y-one

[k]Alternatively C-X-ene-3β,x-diol-y-one

[L]Alternatively C-X-ene-3β,x,y-triol

[m]3β,5β-dihydroxy-B-norcholestane-6β-carboxyaldehyde (aldol) reacts with GP reagent without oxidation by cholesterol oxidase

[n]MS/MS or MS/MS/MS